ELSEVIER

Journal of Quantitative Spectroscopy & Radiative Transfer ▮ (▮▮▮▮) ▮▮▮–▮▮▮

Journal of Quantitative Spectroscopy & Radiative Transfer

www.elsevier.com/locate/jqsrt

Diode laser spectroscopy of CO_2 at 790 nm

A. Lucchesini*, S. Gozzini

Istituto per i Processi Chimico-Fisici del CNR, Area della Ricerca, Via G. Moruzzi 1, I-56124 Pisa, Italy

Received 4 May 2006; received in revised form 9 June 2006; accepted 9 June 2006

Abstract

Absorption lines of $^{12}C^{16}O_2$ have been examined by using a tunable diode laser spectrometer in the region around 12 670 cm^{-1} (790 nm). The spectrometer sources are commercially available double heterostructure InGaAlAs tunable diode lasers (TDLs) operating in the "free-running" mode, which allowed the detection of the line positions within 0.01 cm^{-1}. The observed carbon dioxide absorption lines belong to the combination overtone $2\nu_2 + 5\nu_3$ ro-vibrational band with intensities ranging around 10^{-28} cm/molecule.

Keywords: Carbon dioxide; Overtone absorption spectroscopy; Tunable diode-laser spectrometer

1. Introduction

Diode lasers (DLs) gained a preeminent role as sources for spectroscopy, owing to their easy setup and control and their low cost. The cheapest ones working at room temperature (RT) are those emitting in the visible and the near infrared so that their utilization as spectroscopic tools limits the choice of the samples gases to those which have their vibrational resonances in this spectral range. One of the more interesting of them is carbon dioxide as it is a good sample for the right interpretation of the classical and quantum mechanical behavior of linear symmetric molecules.

The CO_2 overtone resonances have been observed in the near infrared (NIR) spectrum of the atmosphere of the planet Venus, where this molecule is present at 96.5%, by using telescopes, classical spectrographs and photographic plates [1,2]. They have also been analyzed in the laboratory by more and more sophisticated spectroscopic apparatus, starting from classical monochromators, long absorption path lengths and photographic systems [3], then by the photoacoustic detection technique [4] and more recently by the intracavity laser absorption spectroscopy (ICLAS) technique [5] that increases the signal-to-noise ratio (S/N) and permits very precise measurements and spectroscopic predictions [6,7].

Here as a natural continuation of our previous work on the $\nu_1 + 5\nu_3$ ($\Sigma_u^+ \leftarrow \Sigma_g^+$) ro-vibrational combination overtones band of $^{12}C^{16}O_2$ [8] we concentrate our attention on the very weak carbon dioxide band located at about 790 nm, that is the $2\nu_2 + 5\nu_3$ band, where ν_1 is the symmetric stretching, ν_2 the bending and ν_3 the antisymmetric stretching vibrational modes. Our spectroscopic work is based on the utilization of

*Corresponding author. Tel.: +39 0503152532; fax: +39 0503152230.
E-mail address: lucchesini@ipcf.cnr.it (A. Lucchesini).

0022-4073/$ - see front matter © 2006 Published by Elsevier Ltd.
doi:10.1016/j.jqsrt.2006.06.009

commercially available DLs working in the "free-running" regime, that is without any external optical and electrical feedback. DLs have been successfully utilized to study the optical resonances of many molecules, like CH_4, C_2H_2, C_2H_4, CHF_3, CO, CO_2, HF, HCl, H_2O, H_2S, HCN, NH_3, NO, NO_2, O_2, etc. and this list cannot be exhaustive for the increasing utilization of this type of sources. In order to use the frequency modulation (FM) technique they are modulated through their injection current and when the frequency of the modulation is chosen much lower than the resonance line-width, the FM spectroscopy is usually called "wavelength modulation spectroscopy" (WMS). In this work we apply the WMS and the second harmonic detection techniques to the carbon dioxide absorptions around 790 nm, where the $^{12}C^{16}O_2$ ro-vibrational transitions from the fundamental energy level to $(02^05)_1$ {Herzberg notation [9]} (10052) {AFGL HITRAN notation [10,11]} are located.

2. Experimental apparatus and technique

Fig. 1 shows the experimental setup of the diode laser spectrometer. The source is a Fabry–Perot-type semiconductor laser SHARP Mod. LT025MD that emits 40 mW cw single mode at 785 nm at RT without any external optical feedback, i.e. *free-running*. It is driven by a stabilized low-noise Laser Optronic S.p.A. LDD-250D current supply. Its temperature is monitored by a high-stability Laser Optronic bipolar temperature controller LTC-B5A ($\Delta T = 0.01$ K within 1 h). The temperature stabilization of the DL is very important as its emission wavelength is a linear function of the temperature (≈ 0.1 nm/K) but with periodical mode hops. The wavelength scan is obtained by adding a low frequency ($\sim$1 Hz) sawtooth signal to the driving current by a home-made passive mixer. The wavelength dependence on the current is linear (≈ 0.01 nm/mA) for small current variations and is a critical parameter for free-running DL spectroscopy (usual current amplitude values $\sim$ 10–100 mA). The collimated DL radiation is split in different beams, which go through a home-made confocal 5 cm Fabry–Perot interferometer (f.s.r. = 1.5 GHz) to check the frequency sweep and the laser emission mode, and through two Herriott-type multipass cells Mod. MPC-300 by SIT S.r.l., each one giving 30 m path length, one containing the sample gas and the other containing water vapor for checking the eventual H_2O absorptions. The sample gas pressure set between 70 and 100 Torr to give the best S/N ratio in the collected absorption signal. Finally, the laser beam passes through a 1 m iodine closed Pyrex glass cell heated up to 350 K in order to obtain enough vapor pressure for the precise wavenumber reference. The transmitted radiations are collected by pre-amplified silicon photodiodes and the resulting signals are simultaneously acquired by a desk-top computer. A 35 cm focal length monochromator McPherson Mod. 270 is employed for the rough wavelength reading ($\Delta\lambda \simeq 0.01$ nm). A sinusoidal current is mixed to the diode laser injection current for the harmonic detection: the signals transmitted through the cells are sent to the lock-in

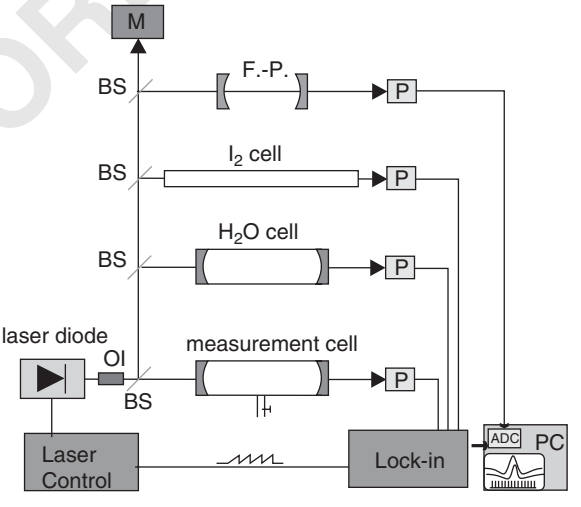

Fig. 1. Outline of the experimental apparatus. BS: beam splitter; F.–P.: Fabry–Perot interferometer; M: monochromator; OI: optical insulator; P: photodiode; PC: desk-top computer.

amplifiers to extract the desired harmonic components. In order to reduce the DL noise an optical insulator is put in front of the DL, which blocks any optical feedback coming from the several windows in the beam path. The carbon dioxide gas was supplied by Praxair Inc. with the following characteristics: grade 4.8 (99.998%), CO <0.5 ppm, $H_2O<3$ ppm, $N_2<10$ ppm, $O_2<2$ ppm, total hydrocarbons <4 ppm.

2.1. Frequency modulation spectroscopy

The intensity of the radiation transmitted through a sample can be written as the product of the incoming intensity $I_0(\nu)$ and the transmittance $\tau(\nu)$, where ν is the distance from the central frequency of the line:

$$I(\nu) = I_0(\nu)\tau(\nu). \tag{1}$$

The transmittance can be described by the Lambert–Beer equation:

$$\tau(\nu) = \mathrm{e}^{-\sigma(\nu)z}, \tag{2}$$

where $z = \rho\, l$ is the column amount (in molecule cm^{-2}), i.e. the product of the absorbing species number density ρ (in molecule cm^{-3}) and the optical path l (in cm) of the radiation through the sample; the absorption cross-section $\sigma(\nu)$ is expressed in cm^2/molecule. In case of weak absorptions, like this case, $\sigma(\nu)z \ll 1$ and Eq. (2) can be approximated by

$$\tau(\nu) \simeq 1 - \sigma(\nu)z, \tag{3}$$

where $\sigma(\nu)$ takes into account the shape of the absorption line: Gaussian for Doppler broadening and Lorentzian for collisional broadening.

In the FM regime the emission frequency of the DL is sinusoidally modulated at frequency $\nu_\mathrm{m} = \omega_\mathrm{m}/(2\pi)$ via the injection current

$$\nu = \bar{\nu} + a\cos\omega_\mathrm{m} t. \tag{4}$$

If the DL emission frequency $\bar{\nu}$ is swept over an interval across the chosen transition, the transmitted signal will depend on both the absorption line shape and the modulation parameters. Since it is an even function of the time, it can be expanded in a cosine Fourier series [12],

$$\tau(\bar{\nu} + a\cos\omega_\mathrm{m} t) = \sum_{n=0}^{\infty} H_n(\bar{\nu}, a)\cos n\omega_\mathrm{m} t, \tag{5}$$

where $H_n(\bar{\nu})$ is the nth harmonic component of the modulated signal. By demodulating the signal with a lock-in amplifier at a multiple $n\nu_\mathrm{m}$ ($n = 1, 2, \ldots$) of the modulation frequency, an output signal proportional to the nth component $H_n(\bar{\nu})$ is collected. When the amplitude a is chosen smaller than the width of the transition line, the nth Fourier component is proportional to the n-order derivative of the original signal,

$$H_n(\bar{\nu}, a) = \frac{2^{1-n}}{n!}\, a^n \left.\frac{\mathrm{d}^n\tau(\nu)}{\mathrm{d}\nu^n}\right|_{\nu=\bar{\nu}}, \quad n \geqslant 1. \tag{6}$$

In this work we detect the second harmonic component ($2f$ detection), which enhances the S/N ratio and reduces to zero the unwanted background.

2.2. High modulation regime

In order to improve the S/N ratio large values of the modulation amplitude are used, but when a is increased, the derivative approximation of Eq. (6) fails and the nth harmonic component $H_n(\nu, a)$ is generally given as [13]

$$H_n(\nu, a) = \frac{2}{\pi}\int_0^{\pi} \tau(\nu + a\cos\theta)\cos n\theta\, \mathrm{d}\theta. \tag{7}$$

The analytical evaluation of this integral is not always possible. Arndt [14] and Wahlquist [15] derived the analytical form for the harmonic components H_n for a Lorentzian absorption function.

An expression for the nth harmonic component can be obtained by inverting Eq. (5)

$$H_n(x,m) = \varepsilon_n \mathrm{i}^n \int_{-\infty}^{+\infty} \hat{\tau}(\omega)\, J_n(m\omega) \mathrm{e}^{\mathrm{i}\omega x}\, \mathrm{d}\omega, \tag{8}$$

where

$$\hat{\tau}(\omega) = \frac{1}{2\pi} \int \tau(x) \mathrm{e}^{-\mathrm{i}\omega x}\, \mathrm{d}x \tag{9}$$

is the Fourier transform of the transmittance profile; $x = v/\Gamma$ and $m = a/\Gamma$ are, respectively, the frequency and the amplitude of the modulation, normalized to the line-width Γ; J_n is the nth order Bessel function; $\varepsilon_0 = 1$, $\varepsilon_n = 2$ $(n = 1, 2, \ldots)$ and i is the imaginary unit.

Let us assume for simplicity a Lorentzian absorption line-shape centered at $v = 0$: this is acceptable when collisional broadening dominates as in our case. Then the cross-section coefficient will be

$$\sigma_{\mathrm{L}}(x,m) \propto \frac{1}{1 + (x + m\cos\omega t)^2}. \tag{10}$$

By referring to the work of Arndt we recalculate the second Fourier component of the cross-section coefficient by putting $n = 2$

$$H_2(x,m) = -\frac{1}{m^2}\left[\frac{\{[(1-\mathrm{i}x)^2 + m^2]^{1/2} - (1-\mathrm{i}x)\}^2}{[(1-\mathrm{i}x)^2 + m^2]^{1/2}} + \text{c.c.}\right] \tag{11}$$

and by eliminating the imaginary part

$$H_2(x,m) = \frac{2}{m^2} - \frac{2^{1/2}}{m^2} \times \frac{1/2[(M^2 + 4x^2)^{1/2} + 1 - x^2][(M^2 + 4x^2)^{1/2} + M]^{1/2} + |x|\,[(M^2 + 4x^2)^{1/2} - M]^{1/2}}{(M^2 + 4x^2)^{1/2}}, \tag{12}$$

where

$$M = 1 - x^2 + m^2.$$

In order to obtain the line position parameters with as maximum accuracy as possible by the WMS technique, we use this function, properly normalized, to fit all the $2f$ spectroscopy observed features by a standard nonlinear least square method. The optimum S/N ratio is obtained when the modulation index $m = 2.2$–2.3 in accordance to what is stated in the literature [14].

3. Experimental results

Forty CO_2 absorption lines are observed and their position measured with $0.01\,\mathrm{cm}^{-1}$ by the comparison with a very precisely known I_2 absorption spectrum [16] and the aid of an I_2 reference cell. Table 1 shows the results with the wavenumbers in vacuum. Since the spin of the O nucleus is zero, the selection rule for the rotational transition permits only absorptions from levels with even J values. The line positions correspond within the errors to the ones reported in HITRAN [11] only up to $J = 22$. Beyond this value the wavenumbers differ more and more.

We observed 80% correspondence in the R-branch and only 40% in the P branch calculated in the work of Campargue et al. [6] by using the energy levels extracted from the available measured spectra, but the correspondences get better when they use the effective Hamiltonian approach [17] and also when they adopt the spectroscopic parameters obtained from the literature [18]. Most of the line positions from the old work of Herzberg [3] match ours within $0.03\,\mathrm{cm}^{-1}$, but others are quite different, due principally to the poor resolving power of his spectrometer that led to a confusion of the CO_2 lines with the close water vapor ones. This is the case of $R(10)$, $P(8)$, $P(10)$ and $P(12)$ where Herzberg writes "blended lines".

Table 1
Measured CO_2 absorption line positions with the difference ($\Delta\nu'$) between this work and HITRAN database [11]

J	$R(J)$ (cm^{-1})	$\Delta\nu'$ (cm^{-1})	σ_{max} ($10^{-26}\,cm^2/mol$)	$P(J)$ (cm^{-1})	$\Delta\nu'$ (cm^{-1})	σ_{max} ($10^{-26}\,cm^2/mol$)
0	12673.03	0.00				
2	12674.45	0.00		12670.70	0.01	
4	12675.75	0.00		12669.00	0.01	
6	12676.93	0.00		12667.16	0.00	0.7 ± 0.1
8	12677.99	0.00	0.8 ± 0.4	12665.23	0.01	0.6 ± 0.1
10	12678.94	0.00	0.5 ± 0.1	12663.17	0.00	0.7 ± 0.1
12	12679.77	0.00	4.6 ± 0.1	12660.99	0.00	1.0 ± 0.2
14	12680.48	−0.01	0.9 ± 0.2	12658.71	0.01	1.0 ± 0.2
16	12681.08	−0.01	1.3 ± 0.4	12656.31	0.01	0.8 ± 0.1
18	12681.56	−0.01	1.2 ± 0.2	12653.77	−0.01	1.6 ± 0.5
20	12681.92	−0.01	1.3 ± 0.4	12651.13	−0.01	1.2 ± 0.1
22	12682.17	−0.01	1.1 ± 0.2	12648.38	0.00	1.3 ± 0.3
24	12682.29	−0.02	0.9 ± 0.2	12645.50	−0.02	1.2 ± 0.3
26	12682.31	−0.02		12642.52	−0.01	0.9 ± 0.1
28	12682.20	−0.03		12639.41	−0.02	
30	12681.96	−0.05		12636.18	−0.03	
32	12681.62	−0.06		12632.84	−0.04	
34	12681.16	−0.07		12629.38	−0.05	
36	12680.57	−0.09		12625.80	−0.06	0.3 ± 0.1
38	12679.88	−0.10		12622.10	−0.09	
40	12679.06	−0.12		12618.28	−0.11	

σ_{max} is the maximum absorption cross-section.
The maximum error (three standard deviations) is $0.01\,cm^{-1}$.

Owing to the derivative spectroscopy method and the high modulation amplitude adopted here, it is difficult to obtain absolute intensity measurements directly from the $2f$ signal. We try to measure the absolute transmission value by direct absorption (DA) with the same long path-length as the WMS one and with a CO_2 pressure around 90 Torr that produces the best S/N and Table 1 gives some results only for the more intense lines. For the weakest absorptions the S/N ratio is so poor that we cannot assert any reliable value of σ_{max} and therefore many intensity values are missing.

The $2f$ spectrum in the region of the R branch turning point is shown in Fig. 2. The folding in the J sequence is due to the decrease of the rotational constant B' with the vibrational excitation. The line positions are identified by using Eq. (12) and a nonlinear fit procedure. The S/N ratio is close to 20 and by considering that here the absorption cross-section is on the order of $10^{-26}\,cm^{-2}$/molecule, it turns out that the spectrometer can detect lines with $\sigma_{max} \approx 10^{-27}\,cm^2$/molecule, which means a minimum detectable absorption intensity $S_{min} \approx 10^{-28}$ cm/molecule in these experimental conditions.

3.1. Determination of the band parameters

In order to obtain the B_v, D_v rotational parameters and v_0 band origin we calculate the combination differences $R(J-1) - P(J+1) = \Delta_2F''(J)$ and the sum $R(J) + P(J)$ [9] from our measurements.

In particular for the B_{000} and D_{000} constants:

$$\Delta_2F''(J) = (4B'' - 6D'')\left(J + \frac{1}{2}\right) - 8D''\left(J + \frac{1}{2}\right)^3 \tag{13}$$

but usually $D''/B'' \approx 10^{-6}$, therefore, Eq. (13) can be written as

$$\Delta_2F''(J) = 4B''\left(J + \frac{1}{2}\right) - 8D''\left(J + \frac{1}{2}\right)^3. \tag{14}$$

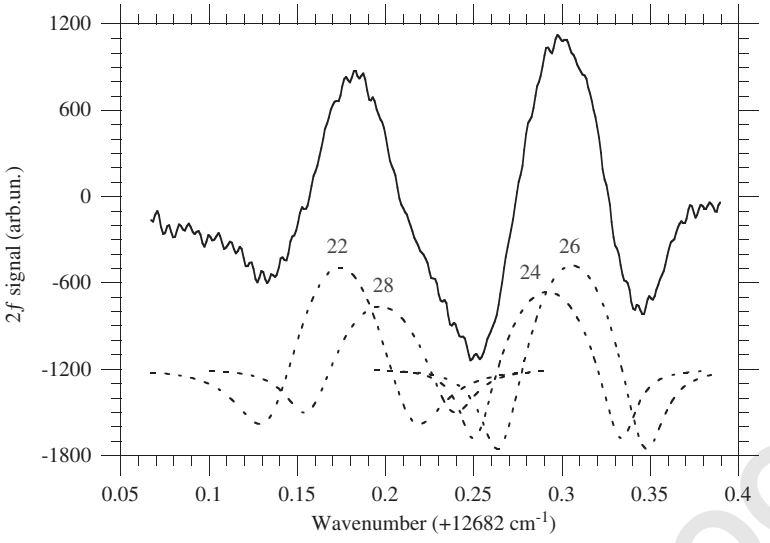

Fig. 2. Second derivative signal of the carbon dioxide transmission spectrum at 788.3 nm obtained by WMS with 10 Hz bandwidth at $p_{CO_2} = 90$ Torr and room temperature. The dotted curves are the ro-vibration resonances as extracted by the fit procedure and are identified by their rotational quantum number.

Table 2
$\Delta_2 F''(J)$ for $2\nu_2 + 5\nu_3$ (this work) and for $\nu_1 + 5\nu_3$ (previous work) [8]

J	$2\nu_2 + 5\nu_3$	$\nu_1 + 5\nu_3$
1	2.33	2.33
3	5.45	5.46
5	8.59	8.59
7	11.70	11.71
9	14.82	14.82
11	17.95	17.95
13	21.06	21.07
15	24.17	24.19
17	27.31	27.30
19	30.43	30.43
21	33.54	33.54
23	36.67	36.67
25	39.77	39.78
27	42.90	42.90
29	46.02	46.02
31	49.12	49.12
33	52.24	52.24
35	55.36	55.36
37	58.47	58.47
39	61.60	61.59
41		64.71
43		67.81
45		70.92
47		74.03

In Table 2 the results of $\Delta_2 F''(J)$ for this work and the ones obtained in our previous one also on $^{12}C^{16}O_2$ [8] are shown together.

After averaging the two sets for each J we plot them as a function of $J(J+1)$ as in Fig. 3. The best linear fit of $\Delta_2 F''(J)/(J+\frac{1}{2})$ vs. $(J+\frac{1}{2})^2$ gives

$$B_{000} = (0.39014 \pm 0.00005)\,\mathrm{cm}^{-1}$$

and

$$D_{000} = (1.1 \pm 0.2) \times 10^{-7}\,\mathrm{cm}^{-1},$$

which is better than the results obtained by Herzberg in 1953 [3] on an average of many more polyads. The errors are the maximum errors (3σ).

Furthermore, to obtain the B_{02^05} and v_0 parameters

$$R(J) + P(J) = 2v_0 + (2B' - 4D') + 2(B' - B'' - 6D')J(J+1) - 2(D' - D'')J^2(J+1)^2, \quad (15)$$

which, following the previous consideration and by taking into account that $D' \simeq D''$, where $''$ stands for the lower and $'$ for the upper state, becomes

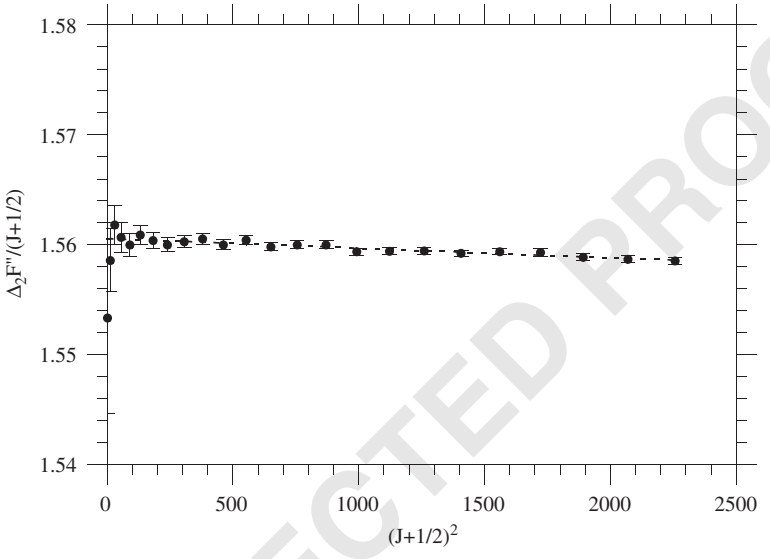

Fig. 3. Plot of $\Delta_2 F''(J)/(J+\frac{1}{2})$ vs. $(J+\frac{1}{2})^2$ along with the best linear fit.

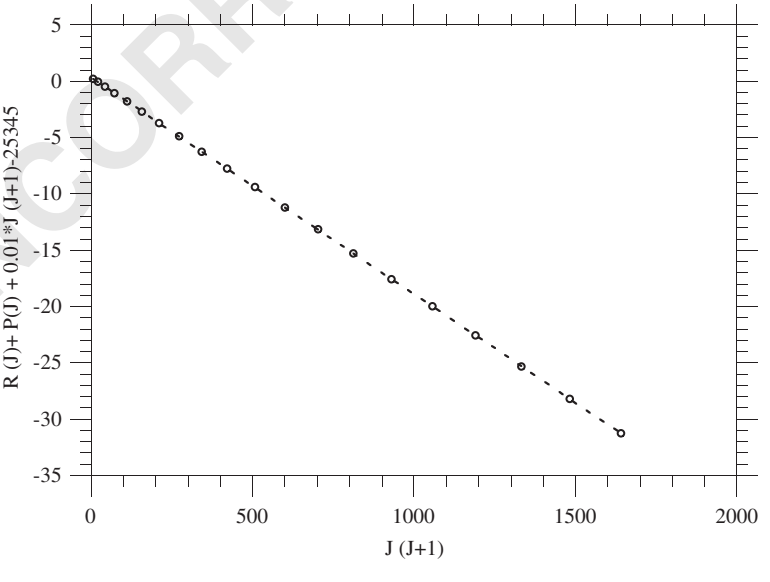

Fig. 4. Plot of $R(J) + P(J)$ vs. $J(J+1)$ along with the best linear fit. The measurement errors are within the empty dots.

$$R(J) + P(J) = 2\nu_0 + 2B' + 2(B' - B'')J(J+1). \quad (16)$$

In Fig. 4, $R(J) + P(J)$ as a function of $J(J+1)$ is shown with the best linear fit. The almost perfect linearity is remarkable (linear regression coefficient $r = 0.9999994$) and confirms our excellent line position accuracy. From the intercept and the angular coefficient and by using the B' value obtained previously we get

$$B_{02^05} = (0.37552 \pm 0.00005)\,\mathrm{cm}^{-1}$$

and

$$\nu_0 = (12672.291 \pm 0.001)\,\mathrm{cm}^{-1},$$

where again the errors are the maximum errors.

The ν_0 parameter matches the one obtained by Campargue et al. [6] within the errors, while B_{02^05} is little lower than theirs.

4. Conclusion

By diode laser WM spectroscopy and the aid of a 30 m total path-length multipass Herriott-type cell, 40 $^{12}C^{16}O_2$ absorption lines have been detected around $12670\,\mathrm{cm}^{-1}$ and their positions measured within $0.01\,\mathrm{cm}^{-1}$. They belong to the combination overtone $2\nu_2 + 5\nu_3$ ro-vibrational band with rotational quantum numbers J up to 40. The absolute line positions have been obtained by comparison with a reference I_2 absorption cell and the utilization of a very precise atlas. The experimental results confirm the wavenumbers listed in HITRAN database for J up to 22, beyond it our experimental results differ more and more, but still conserving an excellent accuracy. The absorption cross-section of the observed lines ranged between 3×10^{-27} and $4.6 \times 10^{-26}\,\mathrm{cm}^2$/molecule at RT and are compatible with HITRAN ones within the errors. The diode laser spectrometer sensitivity permits the observation of absorption lines having intensities of the order $S \approx 10^{-28}\,\mathrm{cm}$/molecule. Care has been taken in the fit of the absorption features by taking into account the distortion caused by the high modulation amplitude adopted for the WM technique. On the base of these measurements, the B_v, D_v rotational parameters and the ν_0 band origin have been obtained.

Acknowledgements

The authors wish to thank Mr. M. Badalassi for the construction of the I_2 reference glass cell, Mr. R. Ripoli for the mechanical constructions and Mr. M. Tagliaferri for the technical support.

References

[1] Adams WS, Dunham Jr. T. Absorption bands in the infra-red spectrum of Venus. Publ Astron Soc Pac 1932;44:243–5.
[2] Gray LD, Schorn RA, Barker E. High dispersion spectroscopic observation of Venus. IV: the weak carbon dioxide band at 7883 Å. Appl Opt 1969;8:2087–93.
[3] Herzberg G, Herzberg L. Rotation–vibration spectra of diatomic and simple polyatomic molecules with long absorbing paths. J Opt Soc Am 1953;43:1037–44.
[4] Yang X, Petrillo CJ, Noda C. Photoacoustic detection of N_2O and CO_2 overtone transitions in the near-infrared. Chem Phys Lett 1993;214:536–40.
[5] Campargue A, Charvat A, Permogorov D. Absolute intensity measurement of CO_2 overtone transitions in the near-infrared. Chem Phys Lett 1994;223:567–72.
[6] Campargue A, Bailly D, Teffo J-L, Tashkun SA, Perevalov VI. The $\nu_1 + 5\nu_3$ dyad of $^{12}CO_2$ and $^{13}CO_2$. J Mol Spectrosc 1999;193:204–12.
[7] Ding Y, Campargue A, Bertseva E, Tashkun SA, Perevalov VI. Highly sensitive absorption spectroscopy of carbon dioxide by ICLAS-VeCSEL between 8800 and $9530\,\mathrm{cm}^{-1}$. J Mol Spectrosc 2005;231:117–23.
[8] Lucchesini A, Gozzini S. Diode laser overtone spectroscopy of CO_2 at 780 nm. JQSRT 2005;96:289–99.
[9] Herzberg G. Infrared and Raman spectra of polyatomic molecules. Princeton, NJ: D. Van Nostrand Co.; 1945.
[10] Rothman LS, Young LDG. Infrared energy levels and intensities of carbon dioxide—II. JQSRT 1981;25:505–24.
[11] Rothman LS, Jacquemart D, Barbe A, Chris Benner D, Birk M, Brown LR, et al. The HITRAN 2004 molecular spectroscopic database. JQSRT 2005;96:139–204.

[12] Reid J, Labrie D. Second-harmonic detection with tunable diode lasers—comparison of experiment and theory. Appl Phys B 1981;26:203–10.

[13] Webster CR, Menzies RT, Hinkley ED. Infrared laser absorption: theory and applications. In: Measures RM, editor. Laser remote chemical analysis. New York: Wiley; 1988.

[14] Arndt R. Analytical line shapes for Lorentzian signals broadened by modulation. J Appl Phys 1965;36:2522–4.

[15] Wahlquist H. Modulation broadening of unsaturated Lorentzian lines. J Chem Phys B 1961;35:1708–10.

[16] Gerstenkorn S, Verges S, Chevillard J. Atlas du spectre d'absorption de la molécule d'iode. Lab. Aimé Cotton, Orsay, France: Editions du CNRS; 1982.

[17] Tashkun SA, Perevalov VI, Teffo J-L, Rothman LS, Tyuterev VIG. Global fitting of $^{12}C^{16}O_2$ vibrational–rotational line positions using the effective Hamiltonian approach. JQSRT 1998;60:785–801.

[18] Rothman LS, Hawkins RL, Wattson RB, Gamache RR. Energy levels, intensities, and linewidths of atmospheric carbon dioxide bands. JQSRT 1992;48:537–66.